Ecosystem properties of semiarid savanna grassland in West Africa and its relationship with environmental variability

Tagesson, Torbern; Fensholt, Rasmus; Guiro, Idrissa; Rasmussen, Mads Olander; Huber, Silvia; Mbow, Cheikh; Garcia, Monica; Horion, Stephanie; Sandholt, Inge; Holm-Rasmussen, Bo; Goettsche, Frank M.; Ridler, Marc-Etienne; Boke-Olén, Niklas; Olsen, Jorgen Lundegard; Ehammer, Andrea; Madsen, Mathias; Olesen, Folke S.; Ardö, Jonas

Published in:
Global Change Biology

DOI:
10.1111/gcb.12734

2015

Document Version:
Publisher's PDF, also known as Version of record

Global Change Biology
celebrating 20 years
Global Change Biology (2015) **21**, 250–264, doi: 10.1111/gcb.12734

Ecosystem properties of semiarid savanna grassland in West Africa and its relationship with environmental variability

TORBERN TAGESSON[1], RASMUS FENSHOLT[1], IDRISSA GUIRO[2], MADS OLANDER RASMUSSEN[13], SILVIA HUBER[13], CHEIKH MBOW[24], MONICA GARCIA[56], STÉPHANIE HORION[1], INGE SANDHOLT[56], BO HOLM-RASMUSSEN[6], FRANK M. GÖTTSCHE[7], MARC-ETIENNE RIDLER[8], NIKLAS OLÉN[9], JØRGEN LUNDEGARD OLSEN[1], ANDREA EHAMMER[1], MATHIAS MADSEN[1], FOLKE S. OLESEN[7] and JONAS ARDÖ[9]

[1]*Department of Geosciences and Natural Resource Management, University of Copenhagen, Øster Voldgade 10, Copenhagen, DK-1350, Denmark,* [2]*Laboratoire d'Enseignement et de Recherche en Géomatique, Ecole Supérieure Polytechnique, Université Cheikh Anta Diop de Dakar, Dakar-Fann, BP 25275, Senegal,* [3]*DHI GRAS A/S, Øster Voldgade 10, Copenhagen, DK-1350, Denmark,* [4]*Research Unit SD6, World Agroforestry Centre, PO Box 30677-00100, Nairobi, Kenya,* [5]*International Research Institute for Climate & Society (IRI), The Earth Institute, Columbia University, Palisades, New York, 10964-8000, USA,* [6]*Technical University of Denmark, Ørsteds Plads 348, Lyngby, DK-2800 Kgs., Denmark,* [7]*Karlsruhe Institute of Technology, Hermann-von-Helmholtz-Platz 1, Eggenstein-Leopoldshafen, 76344, Germany,* [8]*Water Resources Department, Danish Hydrological Institute (DHI), Agern Allé 5, Hørsholm, DK-2970, Denmark,* [9]*Department of Physical Geography and Ecosystem Science, Lund University, Sölvegatan 12, Lund, SE- 223 62, Sweden*

Abstract

The Dahra field site in Senegal, West Africa, was established in 2002 to monitor ecosystem properties of semiarid savanna grassland and their responses to climatic and environmental change. This article describes the environment and the ecosystem properties of the site using a unique set of *in situ* data. The studied variables include hydroclimatic variables, species composition, albedo, normalized difference vegetation index (NDVI), hyperspectral characteristics (350–1800 nm), surface reflectance anisotropy, brightness temperature, fraction of absorbed photosynthetic active radiation (FAPAR), biomass, vegetation water content, and land-atmosphere exchanges of carbon (NEE) and energy. The Dahra field site experiences a typical Sahelian climate and is covered by coexisting trees (~3% canopy cover) and grass species, characterizing large parts of the Sahel. This makes the site suitable for investigating relationships between ecosystem properties and hydroclimatic variables for semiarid savanna ecosystems of the region. There were strong interannual, seasonal and diurnal dynamics in NEE, with high values of ~−7.5 g C m^{-2} day^{-1} during the peak of the growing season. We found neither browning nor greening NDVI trends from 2002 to 2012. Interannual variation in species composition was strongly related to rainfall distribution. NDVI and FAPAR were strongly related to species composition, especially for years dominated by the species *Zornia glochidiata*. This influence was not observed in interannual variation in biomass and vegetation productivity, thus challenging dryland productivity models based on remote sensing. Surface reflectance anisotropy (350–1800 nm) at the peak of the growing season varied strongly depending on wavelength and viewing angle thereby having implications for the design of remotely sensed spectral vegetation indices covering different wavelength regions. The presented time series of *in situ* data have great potential for dryland dynamics studies, global climate change related research and evaluation and parameterization of remote sensing products and dynamic vegetation models.

Keywords: dryland, eddy covariance, evapotranspiration, latent heat flux, net ecosystem exchange, Sahel, savanna, sensible heat flux

Received 7 February 2014; revised version received 12 August 2014 and accepted 14 August 2014

Introduction

Savannas cover approximately one-sixth of the world's land surface and 15.1 million km^2 or 50% of the African continent (Grace *et al.*, 2006). The African Sahel is a region dominated by semiarid grass savannas with shrubs and low tree coverage. Located at the Saharan desert border (Fig. 1), the productivity of these ecosystems is heavily influenced by water availability (Hill & Hanan, 2011). Rainfall declined by ~25% during the 20th century in the region, which is one of the largest

Correspondence: Torbern Tagesson, tel. +46-704 99 39 36, fax +45 35 32 25 01, e-mail: torbern.tagesson@ign.ku.dk

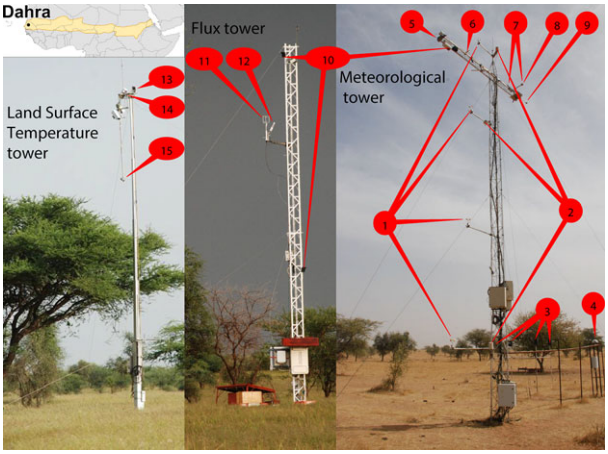

Fig. 1 The set up with the three towers containing all measurement equipment as it was in 2012. In the meteorological tower are (1) the wind speed sensors at four different heights, (2) air temperature and relative humidity sensors at three different heights, (3) rain gauges, (4) the radiometer measuring hyperspectral incoming radiance, (5) the radiometer measuring hyperspectral reflected radiance at seven different angles, (6) grass patch surface infrared temperature sensors, (7) sensors measuring incoming radiation in different wavelength bands, (8) sensors measuring reflected radiation at different angles and different wavelength bands, (9) net radiation sensor, and (10) phenology cameras. In the flux tower are (10) phenology cameras, (11) a sonic anemometer measuring wind speed in three dimensions and (12) an open-path CO_2/H_2O infrared gas analyzer. In the Land Surface Temperature tower are infrared temperature sensors pointing at (13) the sky, (14) a tree crown, and (15) a shaded grass patch. For a complete description of the sensor details, see supplementary material. The photo of the meteorological tower shows the dry season and the photos of the flux and land surface temperature towers show the rainy season. The map indicates the location of the Dahra field site, with the Sahel region being highlighted in orange.

negative trends in the global record (Hulme *et al.*, 2001; Dai *et al.*, 2004; Trenberth *et al.*, 2007). The mean temperature in the region increased by up to 1.3 °C during the same period (Hulme *et al.*, 2001; Trenberth *et al.*, 2007). As a result, the region has experienced several severe droughts since the end of the 1960s (Lebel *et al.*, 2009). However, since the mid-1980s rainfall has steadily increased (Lebel *et al.*, 2009), and there is an ongoing debate whether the region experiences a greening or a browning trend (Dardel *et al.*, 2014). Studies have reported a decline in vegetation productivity (e.g. Adeel *et al.*, 2005), whereas studies based on remotely sensed advanced very high resolution radiometer (AVHRR) data show increased vegetation productivity in the Sahel (e.g. Anyamba & Tucker, 2005; Fensholt *et al.*, 2013).

The population in the Sahel is strongly dependent on rain-fed agriculture and seasonal pasture lands for extensive grazing. The Sahelian dryland ecosystems and its population are thereby particularly vulnerable to land degradation and to the impact of climate variability (Abdi *et al.*, 2014). A range of possible climate feedback mechanisms could arise from these ecosystems, such as changes in albedo, evapotranspiration, and land-atmosphere exchange of carbon dioxide. Future climate scenarios project an increase in temperature and a decrease in rainfall for the western Sahel region (Roehrig *et al.*, 2013). The long-term responses of savanna ecosystems and their resilience to climatic and environmental changes are therefore important to understand, to better quantify and predict the effects of potential climate change.

There are limited *in situ* data available from semiarid savanna grasslands in general and from the African continent in particular. *In situ* data sets from the Sahel covering hydroclimatic variables and ecosystem properties are very rare, and to our knowledge the only sites covering a large array of ecosystem properties are the AMMA-CATCH observatories (Cappelaere *et al.*, 2009; Mougin *et al.*, 2009) and Demokeya (Ardö *et al.*, 2008; Ardö, 2013). *In situ* data are necessary to assess dynamic responses of ecosystems to changing environmental conditions on fine spatial and temporal scales. In addition, *in situ* measurements are important for the parameterization and evaluation of remote sensing products and dynamic vegetation models. Hence, there is an increasing demand for *in situ* data regarding environmental variables and ecosystem properties resulting in research data exchange programs such as SpecNet and FLUXNET (Baldocchi *et al.*, 2001; Gamon *et al.*, 2010).

Remote sensing methods have proven to be a useful tool for studies of ecosystem properties of the Sahel region. There are, however, several sources of uncertainty associated with remote sensing products, such as sensor noise and degradation, calibration errors, atmospheric perturbations (water vapor, aerosols, clouds, scattering, etc.), retrieval algorithm errors, adjacency effects, scaling issues and anisotropic effects. Anisotropic effects are a function of viewing/illumination geometry, and can cause substantial bias in remote sensing products if not accounted for (e.g. Eklundh *et al.*, 2007; Fensholt *et al.*, 2010). However, anisotropic effects can also be seen as an additional information source and it has been shown that the directional properties of vegetated land surface reflectance contain information about vegetation structure (Kimes, 1983; Chen *et al.*, 2003).

To gain insight into properties of semiarid savanna ecosystems and their response to climatic and environmental change, the Dahra field site in Senegal, West Africa, was established as an *in situ* research site in 2002. The main aim of this article is to describe the hydroclimatic conditions (meteorological and hydrological variables) and the ecosystem properties (species composition, albedo, normalized difference vegetation

indices (NDVI), spectral characteristics, surface reflectance anisotropy, fraction of absorbed photosynthetic active radiation (FAPAR), biomass, vegetation water content, and land-atmosphere exchange of energy and carbon) of the site using a unique set of *in situ* data. A further objective is to identify how the dynamics of the ecosystem properties are related to the hydroclimatic variables and to each other.

Materials and methods

Site description

The Dahra field site is located in the semiarid central part of Senegal (15.40°N, 15.43°W) within the Sahelian ecoclimatic zone (Fig. 1). The climate at the site is typical of hot semiarid regions, with daily average air temperature at 2 m height ranging between 15.9 and 39.9 °C (Fig. 2a). Annual rainfall ranged between 169 mm for 2002 and 650 mm for 2010 (Fig. 2c; Table 1), indicating that Dahra experiences a typical sahelian climate, which is defined by the 100 mm and 700 mm isohyets (Prince *et al.*, 1995). More than 95% of the rain falls during the rainy season from July to October, with August being the wettest month. The growing season is relatively short, coinciding with the rainy reason.

The site is a typical low tree and shrub savanna environment with the coexistence of trees and a continuous but strongly seasonal grass cover. In 2008, the tree canopy cover was ~3% of the ground surface with *Balanites aegyptiaca*, *Acacia tortilis*, and *Acacia senegal* as the most dominant species (Table S3) (Rasmussen *et al.*, 2011b). All three tree species exist throughout the Sahel, and *Balanites aegyptiaca*, and *Acacia tortilis* throughout most African arid and semiarid regions (von

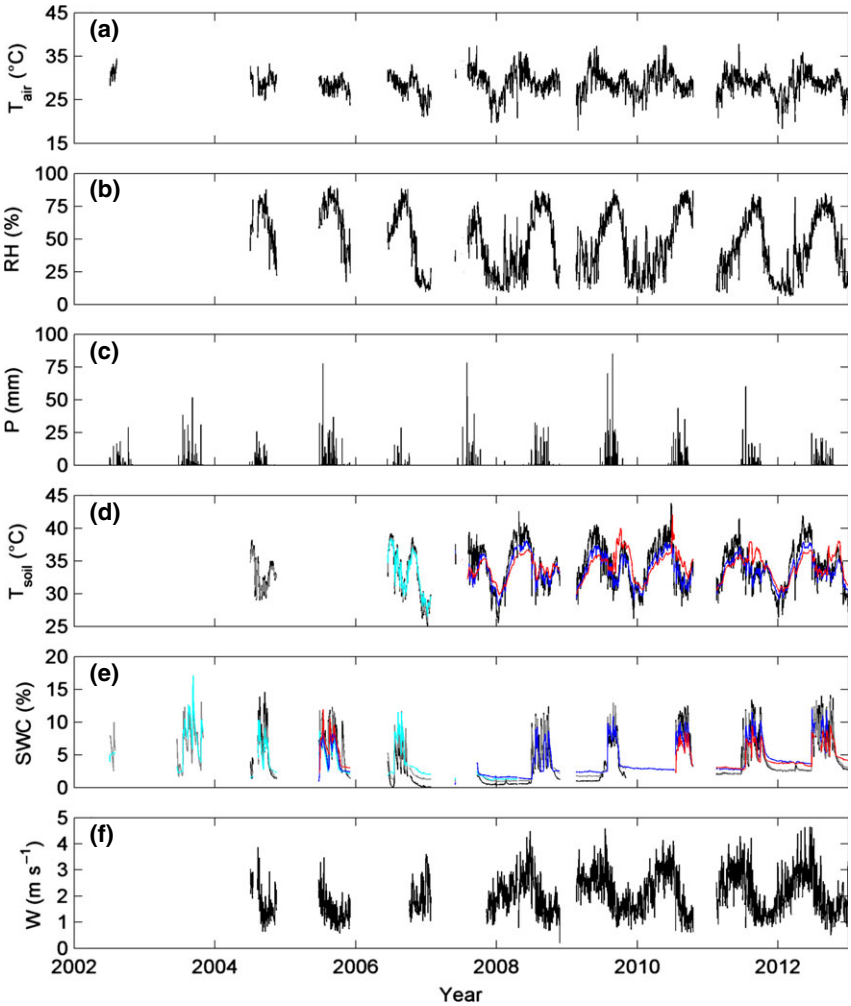

Fig. 2 The hydroclimatic conditions at the Dahra field site 2002–2012; (a) daily averaged air temperature (T_{air}) at ~2 m height (for exact measurement height, see supplementary material), (b) daily averaged relative humidity (RH) at ~2 m height, (c) daily sums of rainfall (P), (d) daily averaged soil temperature (T_{soil}) at 0.05 (black), 0.10 (cyan), 0.15 (gray), 0.30 (blue), and 0.50 (red) m depth, (e) daily averaged soil moisture [SWC, soil volumetric water content (m^3 m^{-3} × 100)] at 0.05 (black), 0.10 (gray), 0.30 (cyan), 0.50 (blue), and 1.00 (red) m depth, and (f) daily averaged wind speed (W) at ~2 m height.

Table 1 Annual values of ecosystem properties and hydroclimatic variables. Start of rainy season is the day of the year (DOY) when the first rain arrived. However, for some years there was a minor rain fall a few weeks before the actual start of the rainy season, a so called false start of the rainy season. These rain falls are not included in the start of the rainy season. End of the rainy season is defined as the last DOY with rain fall. Maximum NDVI is the maximum normalized difference vegetation index. Peak FAPAR is the median fraction of photosynthetically active radiation absorbed by the vegetation for the peak of the growing season. The peak of the growing season was defined as the average of the 15 days around the DOY of maximum NDVI. Maximum biomass and vegetation water content is the maximum value measured. DW is dry weight. – means no data

Year	Annual rainfall (mm)	Start rainy season (DOY)	End rainy season (DOY)	Number of species	Maximum NDVI	Peak FAPAR	Maximum biomass (g DW m^{-2})	Maximum Vegetation water content (%)
2002	169	186	304	–	0.65	–	–	–
2003	346	178	303	–	0.59	–	–	–
2004	323	192	311	–	0.62	–	–	–
2005	488	178	334	–	0.56	0.72	–	–
2006	232	193	279	22	0.82	0.81	150	76
2007	333	191	283	–	0.66	0.67	–	–
2008	302	167	328	31	0.64	0.75	418	68
2009	504	174	274	36	0.59	0.56	289	67
2010	650	174	267	36	0.68	0.62	471	66
2011	486	176	278	35	0.64	0.53	223	73
2012	606	176	289	32	0.61	0.49	206	65

Maydell, 1986). The average tree height was 5.2 m and the breast height diameter was 0.15 m (Table S3). The five most common herbaceous species were *Zornia latifolia*, *Aristida adscensionis*, *Cenchrus biflorus*, *Dactyloctenium aegyptium*, and *Eragrostis tremula*, all of which are found across the western Sahel (a complete description of species composition is given in Table S4). The land is used as grazed rangeland. Effective LAI of the vegetation was measured in 2002 and ranged between 0.05 and 0.79, peaking at the end of August (Figure S2) (Fensholt *et al.*, 2004). The soil is sandy luvic arenosol with negligible amounts of organic material and low clay content (Clay = 0.35%, silt = 4.61%, and sand = 95.04%). To limit the uncertainty in the evaluation and parameterization of remote sensing products and models, criteria for the site selection were that the field site had to be flat with homogeneous vegetation cover within a radius of at least 3 km (Fensholt *et al.*, 2004). The Dahra site is located in the 'Centre de Recherche Zootechnique (CRZ)' managed by the Institut Sénégalais de Recherche Agronomique (ISRA).

The site is equipped with three towers: a meteorological tower with meteorological, hydrological and radiation sensors, a flux tower with an eddy covariance (EC) system for CO_2, H_2O and energy flux measurement, and a land surface temperature tower equipped with infrared thermometers (Fig. 1). A thorough description of measurements of hydroclimatic variables, edaphic conditions, brightness temperature, biomass, species composition, hyperspectral reflectance, and land-atmosphere exchange of CO_2 and energy is given in the supplementary material.

Data analysis

Surface albedo, reflectance, NDVI, and FAPAR. Broadband surface albedo was estimated as reflected total solar irradiance divided by incoming total solar irradiance. The reflectance corresponding to different wavelengths and different viewing angles was estimated by dividing reflected radiance by incoming radiance for each wavelength and angle combination. The reflectance estimates in the near infrared (NIR) and red bands were used to calculate the NDVI as:

$$\mathrm{NDVI} = \frac{\rho_{\mathrm{NIR}} - \rho_{\mathrm{red}}}{\rho_{\mathrm{NIR}} + \rho_{\mathrm{red}}} \quad (1)$$

where ρNIR and ρred are the reflectance in the NIR and the red bands, respectively. The FAPAR was estimated by:

$$\mathrm{FAPAR} = \frac{\mathrm{PAR_{inc}} - \mathrm{PAR_{ref}} - (1 - \alpha_{\mathrm{soil}}) \times \mathrm{PAR_{transmit}}}{\mathrm{PAR_{inc}}} \quad (2)$$

where $\mathrm{PAR_{inc}}$ is incoming photosynthetic active radiation (PAR), $\mathrm{PAR_{ref}}$ is reflected PAR, α_{soil} is PAR albedo of the soil, and $\mathrm{PAR_{transmit}}$ is PAR transmitted through the vegetation.

Surface reflectance anisotropy. To assess the anisotropic effects on the hyperspectral surface reflectance (350–1800 nm), we calculated the anisotropy factor (ANIF) (Sandmeier *et al.*, 1998):

$$\mathrm{ANIF}(\lambda, \theta) = \frac{\rho(\lambda, \theta)}{\rho_0(\lambda)} \quad (3)$$

where ρ is reflectance for the different wavelengths (λ) and the different viewing angles (θ), and ρ_0 is the nadir reflectance. We used the median reflectance for each wavelength (350–1800 nm) measured between 12:00 and 14:00 hours from the peak of the growing season 2011. The peak of the growing season was defined as maximum NDVI ± 7 days.

Land-atmosphere exchange of CO_2 and energy. A complete description of the calculation of the eddy covariance and

gradient estimated fluxes are given in the supplementary material. To be able to estimate daily values of net ecosystem exchange of carbon dioxide (NEE; μmol m^{-2} s^{-1}), sensible heat flux (H; W m^{-2}) and latent heat flux (LE; W m^{-2}), gap-filling is needed. Gaps shorter than and equal to 3 days in NEE were filled using four different approaches: (i) gaps shorter than 2 h were filled using linear interpolation (Falge *et al.*, 2001); (ii) daytime gaps longer than 2 h were filled using the Misterlich function fitted to half-hourly NEE estimates in 7-day gliding windows:

$$\mathrm{NEE} = -(F_{\mathrm{csat}} + R_{\mathrm{d}}) \times (1 - e^{\left(\frac{-\alpha \times \mathrm{PAR}}{F_{\mathrm{csat}} + R_{\mathrm{d}}}\right)}) + R_{\mathrm{d}} \qquad (4)$$

where F_{csat} is the CO_2 uptake at light saturation, R_d is dark respiration and α is the quantum efficiency or the initial slope of the light response curve (Falge *et al.*, 2001); (iii) the night time gaps were filled using average NEE measured during that night; and (iv) remaining gaps were filled using mean diurnal variation 7-day gliding windows (Falge *et al.*, 2001). Gaps in H and LE shorter than 2 h were filled using linear interpolation. Remaining gaps shorter than or equal to 3 days were filled using mean diurnal variation 7-day gliding windows (Falge *et al.*, 2001).

Results and discussions

Species composition

The numbers of grass and herbaceous species identified for the different years ranged between 22 and 36 (Table 1). The interannual variability in number of herbaceous species was correlated with the start of the rainy season and to annual rainfall (Table 2). The year 2006 had the lowest diversity in species composition (Table 1, Table S4). The dominant species in 2006 was

Table 2 Matrix of correlation coefficient (raw 1) and sample size (raw 2) between interannual variation in hydroclimatic variables and ecosystem properties. Rainfall is annual, soil moisture and soil temperature is averaged for the peak of the growing season and measured at 5 cm depth, air temperature and relative humidity were also averaged for the peak of the growing season, and measured at ~2 m height (for exact measurement height, see supplementary material). FAPAR is the median fraction of photosynthetically active radiation absorbed by the vegetation for the peak of the growing season. The peak of the growing season was defined as the average of the 15 days around the DOY of maximum NDVI. The low number of statistically significant correlations is caused by the few number of years measured. Maximum NDVI, biomass and vegetation water content is the maximum values measured. DW is dry weight

	Number of species	Peak Albedo	Maximum NDVI	Peak FAPAR	Maximum Biomass (g DW m^{-2})	Maximum Vegetation water content (%)
Rainfall	0.78	−0.13	−0.39	−0.63	0.30	−0.69
	6	7	11	8	6	6
Soil moisture	0.83*	−0.24	−0.64	−0.35	0.35	−0.28
	6	6	8	7	6	6
Soil temperature	0.40	−0.77	−0.49	−0.81	−0.11	−0.58
	6	6	7	6	6	6
Air temperature	0.80	−0.39	−0.61	−0.78*	0.12	−0.43
	6	6	8	7	6	6
Air humidity	−0.65	0.58	0.31	0.92†	0.05	0.36
	6	6	8	7	6	6
Start of rainy season	−0.98†	0.39	0.57	0.62	−0.49	0.73
	6	7	11	8	6	6
Number of species		−0.32	−0.84*	−0.84*	0.53	−0.62
		6	6	6	6	6
Albedo			−0.34	0.55	−0.15	0.39
			8	8	6	6
NDVI				0.51	−0.30	0.70
				8	6	6
FAPAR					−0.13	0.62
					6	6
Biomass						−0.58
						6

*Statistical significance according a 0.05 threshold.
†Statistical significance according a 0.01 threshold.

an annual legume, *Zornia glochidiata* of the *Fabacea* family, and, in comparison to the other years, only few of the dominant species were annual grasses of the *Poaceae* family (Table S4). Most of the years had a dominant species of the *Zornia* genus. However, under certain rainfall conditions *Zornia glochidiata* can become very dominant and it can produce continuous mats of leaf layers during the rainy season (Burkill, 1995). The year 2006 was the driest of all years, from which species composition was measured, and it also had a so called false start of the rainy season (there was rainfall on ~14 June, 28 days before the main part of the rainy season started). A false start of the rainy season can strongly influence the plant community in that some species (the dominant for the other years) are specialized to grow quickly at the beginning of the rainy season (Elberse & Breman, 1989, 1990; Mbow *et al.*, 2013), and possibly these species did not survive the dry period after the false start of the rainy season. Other factors which were not measured but can strongly influence the species composition in the Sahel are grazing, species composition of the seeds from the previous year, nutrient availability, disturbance history, fire, and herbivory (Hiernaux, 1998; Hérault & Hiernaux, 2004; Hiernaux *et al.*, 2009).

Hyperspectral reflectance

To study the dynamics in spectral reflectance, the ratio between daily median reflectance for each wavelength (350–1800 nm) and the average reflectance for the entire measurement period for each wavelength was calculated (Fig. 3b). As variability in visible (VIS, 350–700 nm) reflectance is mostly affected by changes in leaf pigments (Asner, 1998), there was stronger absorption after bud burst, than at the start of the rainy season and during the dry season (Fig. 3). To reduce excessive heating of the leafs, a large fraction of NIR radiation is reflected in green vegetation and the NIR reflectance is affected mostly by changes in LAI, canopy architecture, and by the spongy mesophyll layer in green leaves (Asner, 1998). The strongest NIR absorption was seen at the end of the rainy season and at the beginning of the dry season, when LAI was at its maximum. The amount of litter decreased over the dry season because of grassing and decomposition and NIR reflectance thereby increased toward the end of the dry season (Fig. 3b). Clear seasonal variation depending on phenology was also visible in the water absorption region around 1450 nm. Reflectance in the short-wave infrared part of the spectrum (1400–1800 nm) was also affected by leaf phenology and vegetation water content, which most likely increased the absorption in these wavelength bands (e.g. Carter, 1991).

Surface reflectance anisotropy

The surface reflectance anisotropy increased with increasing sensor viewing angle for observations made during the rainy season (Fig. 4). With increasing sensor

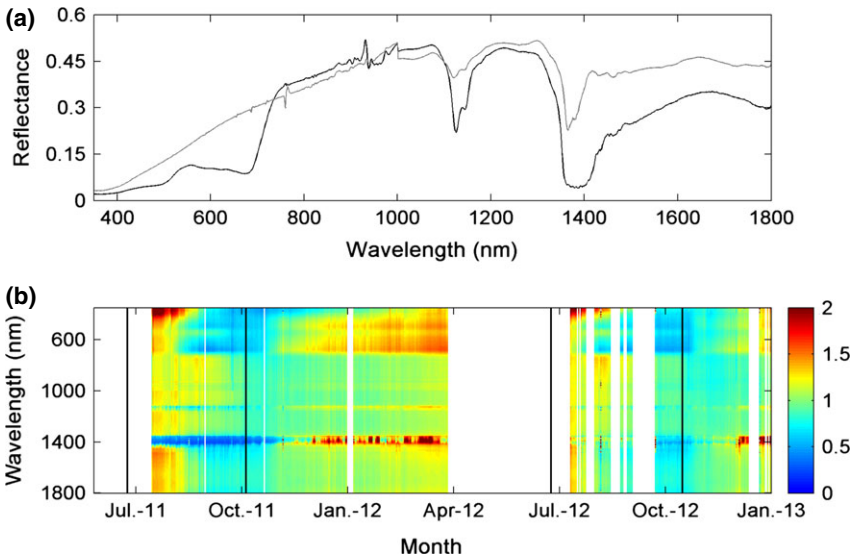

Fig. 3 Reflectance spectrum of the ground surface; (a) median spectra from two different periods are shown, one from the peak of the growing season 2011 with dense vegetation (black) and one from the dry season 2012 (day of year 71–85) with sparse or no vegetation (gray). (b) The ratio between daily median reflectance for each wavelength (350–1800 nm) and the average reflectance for the entire measurement period 2011–2012 for each wavelength. The black lines in (b) indicate the start and end of the rainy seasons (first and final day of rainfall). Only data measured with the sensor pointing nadir were used.

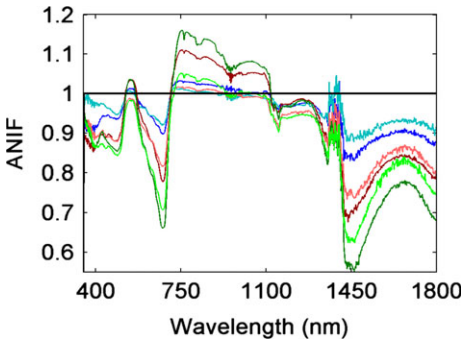

Fig. 4 Surface reflectance anisotropy factors (ANIF) for the wavelengths between 350 and 1800 nm measured at the peak of the growing season 2011. The different lines are nadir (black), 15°W (dark blue), 15°E (light blue), 30°W (dark red), 30°E (light red), 45°W (dark green), 45°E (light green).

viewing angle, more top of the vegetation canopy is viewed and soil and shading effects decrease, which thereby increases ANIFs with sensor viewing angle (Kimes, 1983). The ANIF for the blue, red and the SWIR bands were less than one whereas the ANIF for green and NIR were close to or exceeded the nadir value of 1. Green plant leaves absorb incident energy in the blue, red, and SWIR wavelengths, while the green and NIR energy is mostly reflected or transmitted in the mesophyll of the plant material (Kimes, 1983). The shift in anisotropy for different wavelength regions could have implications for the design of remotely sensed spectral vegetation indices covering different wavelengths.

For most years, there was an effect of surface reflectance anisotropy on NDVI at the Dahra site (Figure S1). Generally, NDVI increases with viewing angle as only the top part of the canopy is seen (Kimes, 1983) whereas soil background has a larger influence for the nadir pointing estimates (Fensholt *et al.*, 2006). This mainly affects the NDVI for larger viewing zenith angles (Huber *et al.*, 2014), which explains why the NDVI measured at 22.5° and 23° off-nadir viewing angles were most similar to the nadir estimates. Measuring with a hemispherical sensor not only increases the footprint but also adds this effect to the NDVI estimates, explaining the slightly higher NDVI values for the hemispherical sensor. No anisotropic effects were seen for the years 2004 and 2005. Unfortunately, we do not have species composition estimates from these years and we do not have NDVI obtained at different sensor viewing angles from 2006. It could be that the

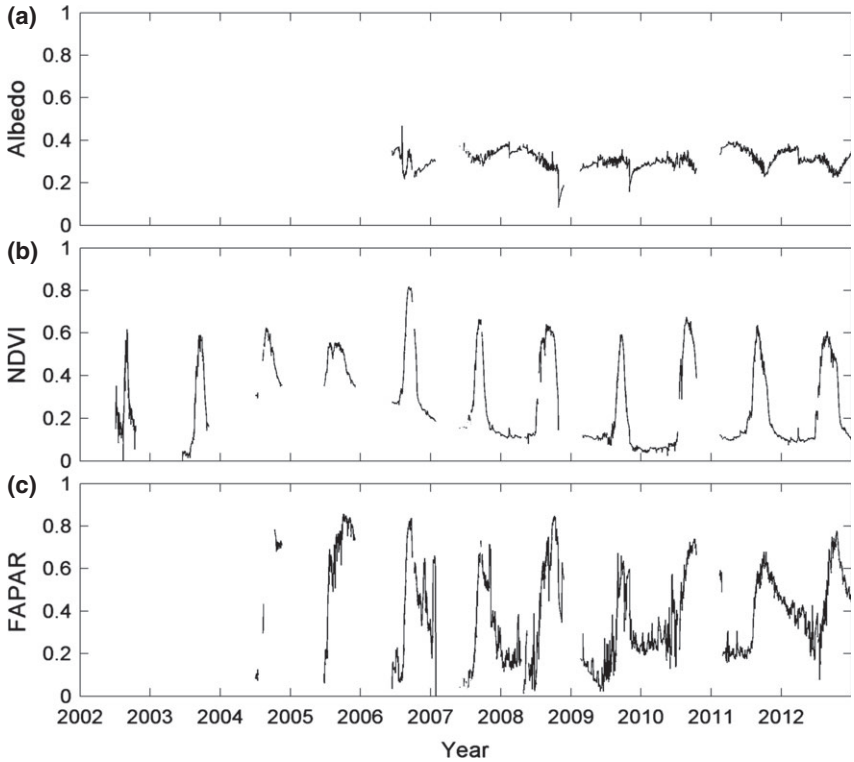

Fig. 5 Time series 2002–2012 of albedo, NDVI, and FAPAR; (a) daytime median albedo, (b) daytime median normalized difference vegetation index (NDVI) measured at nadir hemispherically with a Moderate Resolution Imaging Spectroradiometer (MODIS) sensor response configuration (from which the longest time series is available), and (c) daytime median fraction of photosynthetically active radiation absorption (FAPAR). The median values were taken from between 10:00 and 16:00 hours for each day.

years 2004 and 2005 were dominated by planophile species, as was 2006, whereas the other years were dominated by erectophile species. Planophile species show weaker anisotropic effects than erectophile species (Kimes, 1983).

Albedo, NDVI, and FAPAR

The annual variability in the daily albedo (median value between 10:00 and 16:00 hours) was distinct, with values between 0.25 and 0.4. There was a clear effect of ground vegetation on surface albedo (Fig. 5a). During dry seasons, albedo was similar to desert sand of the Sahara (0.4) (Tetzlaff, 1983), whereas during the growing season it was similar to grass (0.25) (Jones & Vaughan, 2010), and values were within the range typical of other sites in the Sahel (Samain *et al.*, 2008; Mougin *et al.*, 2009).

NDVI ranged between 0.02 and 0.82, with strong seasonal dynamics following the phenology of the green vegetation (Fig. 5b). The highest and lowest maximum NDVI were measured in 2006 and 2005, respectively (Table 1). There was strong interannual variability in dry season NDVI (Fig. 5b), which can be explained by variability in the signal from surrounding evergreen trees and remaining dry biomass during the dry season.

June 3 2009 had the largest fraction of PAR_{inc} transmitted to the soil (99.6%). Median PAR albedo measured between 10:00 and 16:00 hours that day (0.20) was assumed to be the α_{soil} and used in the FAPAR calculations [Eqn (2)]. The FAPAR ranged between 0.01 and 0.86, with high values at the rainy season and low values during the dry season (Fig. 5c).

Time series of vegetation indices are the main tool for detecting trends in land surface condition of drylands using remote sensing (e.g. Tucker *et al.*, 1991; Prince & Goward, 1995; de Jong *et al.*, 2013; Dardel *et al.*, 2014). There are reports of declining vegetation productivity since the mid-1980s (Adeel *et al.*, 2005; Cappelaere *et al.*, 2009), whereas others found a greening trend of the Sahel for the same period (e.g. Eklundh & Olsson, 2003; Anyamba & Tucker, 2005; Mougin *et al.*, 2009; Fensholt *et al.*, 2013; de Jong *et al.*, 2013). For the AMMA-CATCH observatory in Niger, Cappelaere *et al.* (2009) attributed the decreased vegetation productivity to the strong human impact (land use change, increased grazing, wood cutting, and decreased fertility) affecting the land, whereas de Jong *et al.* (2013) showed that greenness trends in the Sahel region were explained by climatic effects. Based on AVHRR data for the period 2002-2011, Dardel *et al.* (2014) showed a greening trend for the Gourma region in Mali, explained by that the vegetation reacted to more favorable rainfall. However, they showed a browning trend for the Fakara region in Niger, possibly explained by a reduction in available land for pastoral use and a decline in soil fertility. At Dahra no trend in maximum *in situ* NDVI was observed between 2002 and 2012 [sample size 11, Sen's slope 0.0002 (not significant at 95% confidence interval)], i.e. there was no browning or greening trend (Fig. 5b). During this period, there was an increasing trend in rainfall (Sen's slope 23.87 mm yr^{-1}), but it was not significant. There were no clear trends in the other hydroclimatic variables (Fig. 2).

There were strong negative correlations between both maximum NDVI and peak of the growing season FAPAR with the number of species (Table 2). This was due to the year 2006 where *Zornia glochidiata* was the dominant species covering the ground with thick planophile leaves, which led to high values of NDVI, leaf area index (LAI) and FAPAR while at the same time reducing the number of species considerably (Mbow *et al.*, 2013).

There was no connection between either soil moisture or annual rainfall and maximum NDVI and peak of the growing season FAPAR (Table 2), which is surprising given the well-documented correlation between primary productivity and rainfall for semiarid savanna ecosystems in general (e.g. Hill & Hanan, 2011). A possible explanation can be alleviated water stress

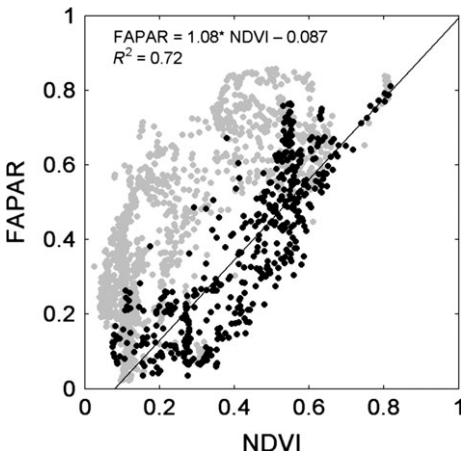

Fig. 6 The relationship between FAPAR and NDVI. FAPAR is fraction of absorbed photosynthetically active radiation and NDVI is normalized difference vegetation index. Gray dots are measured during the dry season and after the day of year with maximum NDVI, whereas black dots are measured from the start of the rainy season and until the day of year with maximum NDVI. The rainy season is defined to start the first day of year when it rains. However, for some years there was a minor rainfall a few weeks before the actual start of the rainy season, a so called false start of the rainy season. These rainfalls are not included in the rainy season.

conditions for vegetation growth; rainfall has been relatively high during the study period, and during the rainy seasons soil moisture was always above the permanent wilting point (2.78%), indicating no water stress for the plants. On the other hand, peak of the growing season FAPAR was strongly negatively correlated with peak of the growing season air temperature and strongly positively correlated with peak of the growing season air humidity (Table 2). This may indicate that for high temperatures and low air humidity, plants close their stomata to limit water losses, while at the same time reducing PAR absorption.

Several studies from semiarid areas and other ecosystem types have shown linear correlations between FAPAR and NDVI (e.g. Myneni & Williams, 1994; Fensholt *et al.*, 2004; Tagesson *et al.*, 2012). Our result only showed a weak nonsignificant correlation between annual maximum NDVI and the peak of the growing season FAPAR (Table 2). However, the correlations in the cited studies were based on seasonal variation in FAPAR by the photosynthetic tissues. We measured FAPAR for the entire plant community, and it was linearly correlated with NDVI during the vegetative phase (beginning of the growing season until the day of year (DOY) with maximum NDVI), but not during senescence and the dry season (Fig. 6). During the vegetative phase basically all PAR was absorbed by the green vegetation, which explains why the two metrics correlate well during this part of the phenological development. Our results highlight potential difficulties when using

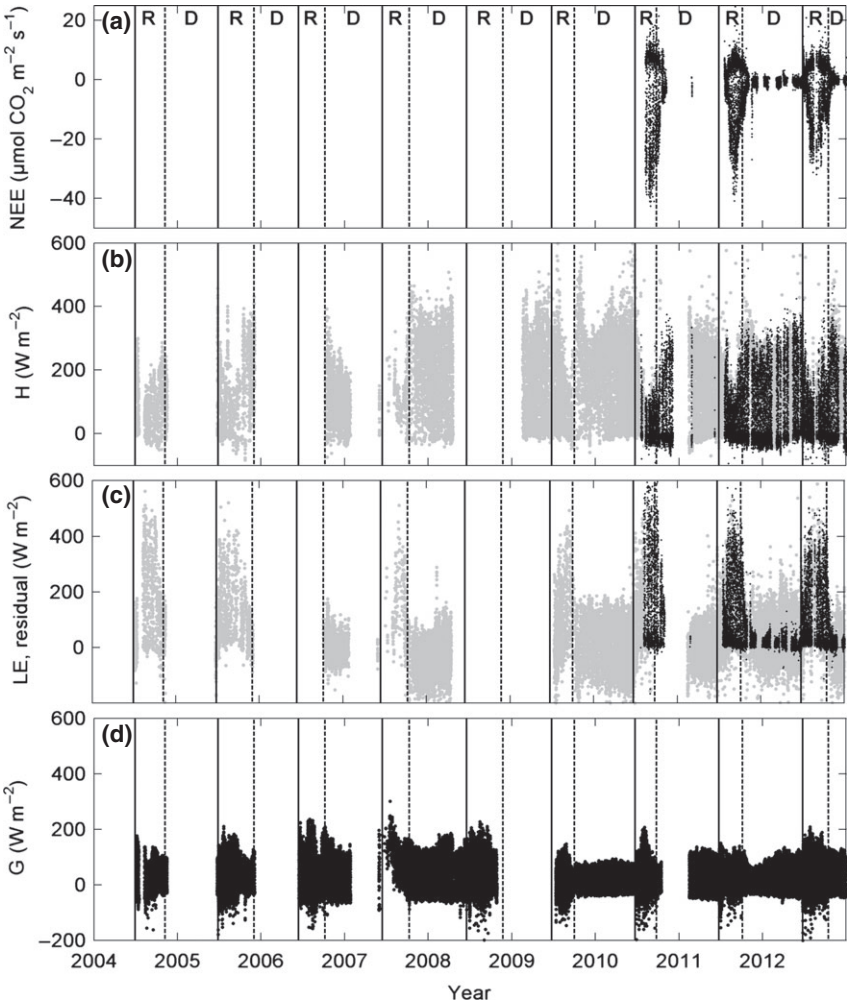

Fig. 7 Half-hourly estimates of land-atmosphere exchange of carbon dioxide and energy; (a) net ecosystem exchange of CO_2 (NEE) 2010–2012; (b) sensible heat flux (H) 2004–2012 measured with the eddy covariance (EC) method (black dots), and the gradient method (gray dots); (c) latent heat flux (LE) measured with the EC method (black dots), and residuals (net radiation – H – ground heat flux) measured with the gradient method (gray dots); and (d) ground heat flux (G) 2004–2012. The full lines indicate the start (first day of rainfall) and the dotted lines indicate the end of the rainy seasons (final day of rainfall). R means rainy season and D means dry season.

remotely sensed NDVI for estimating FAPAR over a full growing season including the period of senescence. There is an ongoing debate within the FAPAR community, whether FAPAR should be measured for the entire plant or if a method for estimating FAPAR for the green fraction of the vegetation only should be defined (CEOS LPV FAPAR sub-group, 2014).

Properties of the grass and herbaceous vegetation

Vegetation water content was highest in 2006 and lowest in 2012, whereas the lowest and highest amount of dry biomass was measured in 2006 and 2010, respectively (Table 1, Figure S3). There were no correlations between maximum aboveground biomass and any of the environmental variables (Table 2). In 2008 and 2010 there was substantially more maximum biomass in comparison to the other years (Table 1), yet none of the measured environmental variables deviate for these years in comparison to the other years. We can thereby not draw any conclusion about what caused these high productivity years. Factors that were not measured but can cause interannual variability in biomass are grazing, disturbance, or herbivory (Hiernaux, 1998; Hérault & Hiernaux, 2004; Hiernaux *et al*., 2009). Biomass was similar to that at other Sahelian sites for all years except these two peak years (Mougin *et al*., 2009).

Remotely sensed NDVI and FAPAR is often used as input data to estimate biomass and vegetation productivity (e.g. Boelman *et al*., 2003; Tagesson *et al*., 2012). However, our results indicate no such relationships (Table 2). Again, the explanation could be the species *Zornia glochidiata*, a planophile annual legume covering the surface with thick leaves: this increased the LAI, NDVI, and FAPAR, but since these species do not grow very high, they have a low biomass. The profound effect that the interannual variability in species composition has on the relationship between vegetation indices (NDVI, FAPAR, and LAI) and biomass/NPP poses a substantial challenge to accurate satellite-based biomass/NPP estimates in drylands using production efficiency models based on input from optical remote sensing (Mbow *et al*., 2013). Another factor influencing NPP and biomass is the dependence of most herbaceous species on previous year's seeds, and herbivory or rainfall can have strong effects on the seed stocks (Hiernaux *et al*., 2009; Mougin *et al*., 2009).

Net ecosystem exchange of carbon dioxide

Strong interannual, seasonal, and diurnal dynamics in CO_2 flux were seen in NEE (Fig. 7a). The fluxes were highest during the rainy season (average NEE −1.9 g C m^{-2} day^{-1}) and lowest during the dry season (average NEE −0.2 g C m^{-2} day^{-1}). NEE peaked at ~—7.5 g C m^{-2}°day^{-1} during the growing season 2010, which was considerably higher than for other studied semiarid sites in Africa (Verhoef *et al*., 1996; Veenendaal *et al*., 2004; Brümmer *et al*., 2008; Kutsch *et al*., 2008; Boulain *et al*., 2009; Sjöström *et al*., 2009). For most of these sites, lower rainfall, lower LAI, or sparser vegetation could possibly explain lower NEE values (Verhoef *et al*., 1996; Veenendaal *et al*., 2004; Boulain *et al*., 2009; Sjöström *et al*., 2009). However, the study sites of Kutsch *et al.* (2008) and Brümmer *et al.* (2008) had similar or larger amounts of rainfall and LAI than Dahra, but they also had higher fluxes than at the other sites, but they were still substantially lower than at Dahra. The level of the NEE values at Dahra were instead similar to the level of tropical C4 wetland plants, humid tropical grassland, and temperate C4 grassland species (Kim *et al*., 1992; Dugas *et al*., 1999; Morison *et al*., 2000; Merbold *et al*., 2009; Saunders *et al*., 2012). Several factors can substantially impact the observed fluxes, such as radiation regime, soil type, site history (cultivation, fire sequences, and disturbances), vegetation age, species composition, and moisture and nutrient conditions (Hill & Hanan, 2011). The soil nutrient concentration was indeed relatively high in the area (0. 40 ± 0.10 mg N g^{-1} soil; 3.2 ± 1.0 g C kg^{-1} soil at 0–20 cm depth in February 2011).

Half-hourly NEE was strongly correlated with PAR following the Misterlich light response function [Eqn (4); Fig. 8; Table 3] for all days except DOY 158, and DOY 177–179 in 2012. PAR is a strong factor controlling photosynthesis (e.g. Lambers *et al*., 1998; Tagesson & Lindroth, 2007), and it overruled the influence of all other environmental variables on half-hourly NEE. At DOY 158 in 2012, during the end of the dry season, there was only little vegetation productivity. At the beginning of the rainy season (DOY 177–179, 2012), just after the first rainfall, there was a large positive burst in

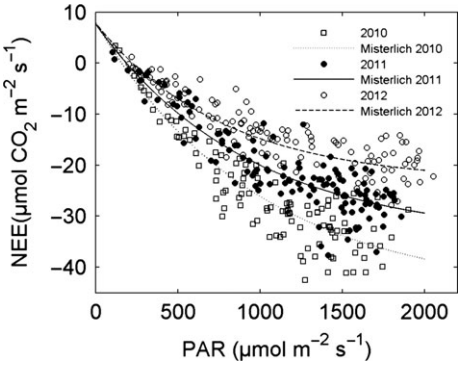

Fig. 8 The relationship between NEE and PAR. Daytime half-hourly net ecosystem exchange (NEE) against incoming photosynthetically active radiation (PAR) for the 7-day period at the peak of 2010, 2011, and 2012. The lines are the fitted Misterlich light response curves [Eqn (4) in the text]. The fitted parameters are given in Table 3.

Table 3 The fitted parameters of the light response function [Eqn (4) in the main text] for the peak of the growing season 2010, 2011, and 2012. F_{csat} is the CO_2 uptake at light saturation (μmol CO_2 μmol m^{-2} s^{-1}), R_d is dark respiration (μmol CO_2 μmol m^{-2} s^{-1}) and α is the quantum efficiency or the initial slope of the light response curve (μmol CO_2 μmol PAR^{-1}) (Falge *et al.*, 2001)

Year	F_{csat}	R_d	α
2010	45.3	7.9	0.054
2011	34.2	7.7	0.045
2012	23.4	7.8	0.040

CO_2 flux indicating a strong increase in ecosystem respiration (CO_2 uptake being defined as negative and CO_2 release as positive). This ecosystem respiration flux masked the minor vegetation productivity at the beginning of the growing season, which explains the lack of correlation between NEE and PAR for this period.

Brightness temperatures

There are relatively large differences in daily averages of brightness temperature (BT) for the three present surface types, i.e. the sunlit and shaded patches containing a mixture of grass and soil and the tree crown (Fig. 9). As to be expected, the unshaded grass and soil patch showed the largest diurnal and seasonal variability, with the highest temperatures during dry seasons when solar exposure was highest (early summer). During the rainy season, the variation in BT was much lower due to the dense grass cover and availability of moisture at the surface for evapotranspiration. For the shaded grass and soil patch and for the (evergreen) tree crown, the seasonal variation in BT was much lower and the two had almost identical BT during the dry season whereas the tree canopy was generally slightly cooler than the shaded grass patch during the rainy season. The availability of measurements from three different surface types, combined with detailed spatial information about the surroundings, provide a unique dataset for evaluating large scale satellite-based land surface temperature products in a savanna landscape (Rasmussen *et al.*, 2011a).

Energy fluxes

H was lower during the rainy season (EC estimated average H: 28 W m^{-2}) than in the dry season (EC

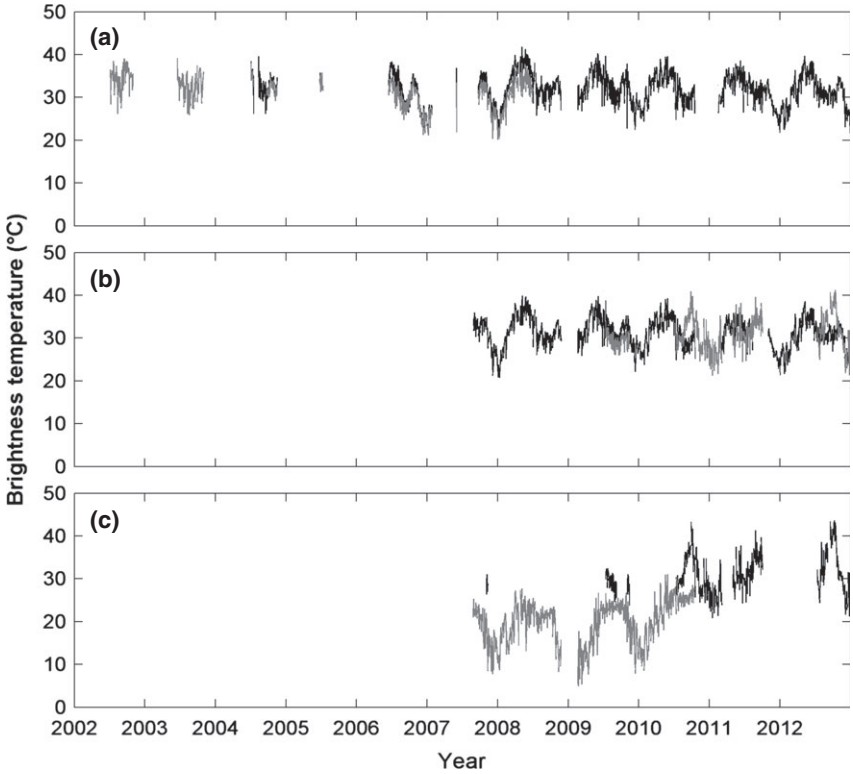

Fig. 9 Time series of daily average brightness temperature (BT) 2002–2012; (a) measured with Raytek Miniature Infrared (MI) sensors at 23° off-nadir angle toward NW (black) and at nadir (gray) at a sunlit grass patch, (b) measured with Apogee Precision Infrared Thermocouple Sensors (IRTS-P) at 23° off-nadir angle toward NW at a sunlit grass patch (black) and at a shaded grass patch, and (c) measured with IRTS-P sensors at a tree crown (black) and at the sky (gray) pointing at 127° off-nadir angle toward N.

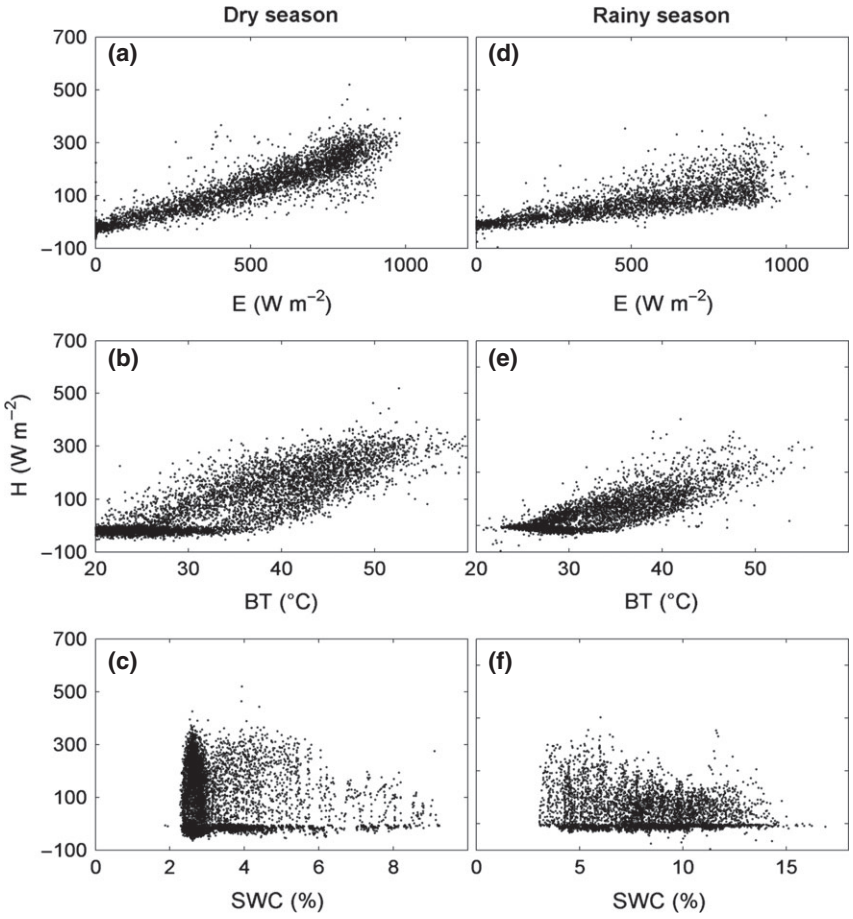

Fig. 10 Sensible heat flux (H) against environmental variables; H measured with the eddy covariance method against solar radiation (E), brightness temperature (BT) and soil moisture at 5 cm depth [SWC, soil volumetric water content (m^3 m^{-3} × 100)] for the dry and rainy season.

estimated average H: 54 W m^{-2}), whereas LE was higher during the rainy season (EC estimated average LE: 122 W m^{-2}) in comparison to the dry season (EC estimated average LE: 47 W m^{-2}) (Fig. 7b and c). The measured values of the energy fluxes and their temporal patterns were similar to other savanna sites (e.g. Ardö *et al.*, 2008; Brümmer *et al.*, 2008; Mougin *et al.*, 2009).

Previously it has been found that H and LE are strongly affected by phenology, soil type, lateral water distribution, and surface temperature (e.g. Stisen *et al.*, 2008; Cappelaere *et al.*, 2009; Timouk *et al.*, 2009). LE and H were coupled to phenology and rainfall patterns also at the Dahra site: LE was considerably higher, whereas H was lower during the rainy season than during the dry season (Fig. 7b and c). H was strongly affected by solar irradiance and brightness temperature (Fig. 10a, b, d, and e). The large scatter could be due to the long period included in the relationships (giving diurnal-, intra-, and interannual variability 2010–2012) and variability in other environmental variables affecting the fluxes. There was a boundary line for maximum H set up by soil moisture, since at high soil moisture values potential H decreased as more energy was used for LE (Fig. 10c and f). There was no difference in the relationships between H and environmental variables for the rainy and dry season. None of the environmental variables alone could explain LE, yet still affecting it by setting potential boundary lines (Fig. 11). Surprisingly, LE was not correlated with soil moisture at 0.05 m depth. An explanation could be direct wet soil and canopy evapotranspiration of minor rainfall events that do not increase the soil moisture at 0.05 m depth.

Theoretically, the residual of the energy balance (net radiation – H – ground heat flux) should be attributed to the LE (when LE is not measured) and it is often used as a proxy for evapotranspiration in model evaluations (e.g. Stisen *et al.*, 2008). However, LE and the residual are not measuring the same. A comparison between eddy covariance estimated LE and gradient estimated residuals generated a root mean square error

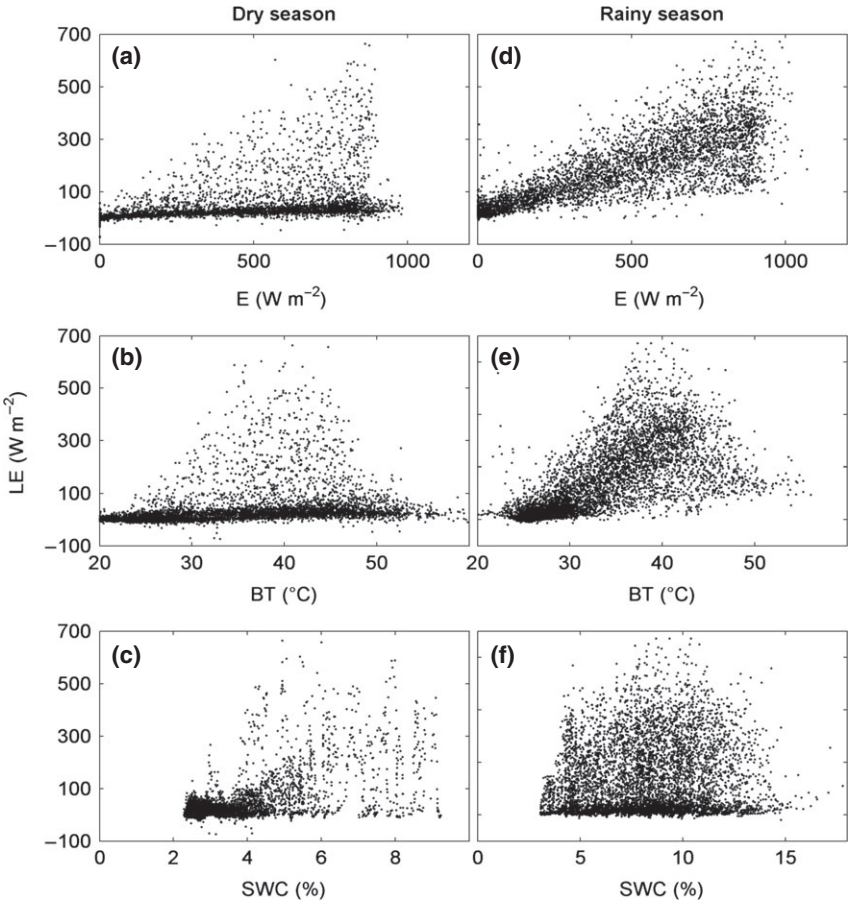

Fig. 11 Latent heat flux (LE) against environmental variables; LE measured with the eddy covariance method against solar radiation (E), brightness temperature (BT), and soil moisture at 5 cm depth [SWC, soil volumetric water content (m^3 m^{-3} × 100)] for the dry and rainy season.

of 103 W m^{-2} (supplementary material), and it can be seen that the residuals reached values up to ±200 W m^{-2} during the dry season (Fig. 7c). LE should be low during the dry season according to both the eddy covariance measured LE and other studies in semiarid savanna ecosystems (Veenendaal *et al.*, 2004; Ardö *et al.*, 2008; Brümmer *et al.*, 2008). This indicates that the residual of the energy budget (net radiation – H – ground heat flux) cannot be attributed to LE entirely. A 100% energy budget closure is usually not achieved and even for eddy covariance systems gaps of ±20% are observed widely (Moncrieff *et al.*, 1997). The large negative residual values in the gradient method were thereby not caused by dew formation, but deviations in the energy budget. Reasons for the deviations could be different footprints of sensors, advective fluxes, energy storage, and measurement errors. This indicates that the residual approach for estimating LE should be used with caution.

A comparison between eddy covariance estimated and gradient estimated H indicated root mean square errors of 42.0 W m^{-2} (supplementary material). Fluxes estimated by the gradient approach are highly sensitive to instrumentation errors and a 1 °C error in vertical temperature difference can result in flux errors as high as 100% (Brotzge & Crawford, 2000). However, the scatter appears random and no systematic bias was observed (Figure S5). When averaged daily or over longer periods, the flux estimates can thereby still be valuable for the evaluation of dynamic vegetation models or remote sensing products. It will thereby contribute to advancing research in Earth observation, biogeochemical cycling, dryland degradation, and the interaction between the semiarid savanna grassland ecosystems. As will the rest of this unique *in situ* data set.

Acknowledgements

The project was funded by the Danish Council for Independent Research (DFF) Sapere Aude programme. Faculty of Science, Lund University supported the measurements with an

infrastructure grant. We are very grateful to the Institut Des Sciences de l'Environnement at the University of Dakar and to the Institut Senegalais de Recherche Agricole for all logistic, administrative and technical support. We thank the reviewers for very constructive and thorough reviews.

References

Abdi A, Seaquist J, Tenenbaum D, Eklundh L, Ardö J (2014) The supply and demand of net primary production in the Sahel. *Environmental Research Letters*, **9**, 094003.

Adeel Z, Safriel U, Niemeijer D, White R (2005) *Ecosystems and Human Well-Being: Desertification Synthesis; a Report of the Millennium Ecosystem Assessment*. World Resources Institute, Washington, DC, pp. 1–26.

Anyamba A, Tucker CJ (2005) Analysis of Sahelian vegetation dynamics using NOAA-AVHRR NDVI data from 1981 to 2003. *Journal of Arid Environments*, **63**, 596–614.

Ardö J (2013) A 10-year dataset of basic meteorology and soil properties in Central Sudan. *Dataset Papers in Geosciences*, **2013**, 6.

Ardö J, Mölder M, El-Tahir B, Elkhidir H (2008) Seasonal variation of carbon fluxes in a sparse savanna in semi arid Sudan. *Carbon Balance and Management*, **3**, 7.

Asner GP (1998) Biophysical and biochemical sources of variability in canopy reflectance. *Remote Sensing of Environment*, **64**, 234–253.

Baldocchi D, Falge E, Gu L *et al.* (2001) FLUXNET: a new tool to study the temporal and spatial variability of ecosystem-scale carbon dioxide, water vapor, and energy flux densities. *Bulletin of the American Meteorological Society*, **82**, 2415–2434.

Boelman NT, Stieglitz M, Rueth HM, Sommerkorn M, Griffin KL, Shaver GR, Gamon JA (2003) Response of NDVI, biomass, and ecosystem gas exchange to long-term warming and fertilization in wet sedge Tundra. *Oecologia*, **135**, 414–421.

Boulain N, Cappelaere B, Ramier D *et al.* (2009) Towards an understanding of coupled physical and biological processes in the cultivated Sahel – 2. Vegetation and carbon dynamics. *Journal of Hydrology*, **375**, 190–203.

Brotzge JA, Crawford KC (2000) Estimating sensible heat flux from the Oklahoma Mesonet. *Journal of Applied Meteorology*, **39**, 102–116.

Brümmer C, Falk U, Papen H, Szarzynski J, Wassmann R, Brüggemann N (2008) Diurnal, seasonal, and interannual variation in carbon dioxide and energy exchange in shrub savanna in Burkina Faso (West Africa). *Journal of Geophysical Research*, **113**, G02030.

Burkill HM (1995) *The Useful Plants of West Tropical Africa*, vol. **3**. Royal Botanic Gardens, Kew, pp. 1–857.

Cappelaere B, Descroix L, Lebel T *et al.* (2009) The AMMA-CATCH experiment in the cultivated Sahelian area of south-west Niger – Investigating water cycle response to a fluctuating climate and changing environment. *Journal of Hydrology*, **375**, 34–51.

Carter GA (1991) Primary and secondary effects of water content on the spectral reflectance of leaves. *American Journal of Botany*, **78**, 916–924.

CEOS LPV FAPAR sub-group (2014) First Workshop CEOS LPV FAPAR sub-group. Available at: http://fapar.jrc.ec.europa.eu/WWW/Data/Pages/FAPAR_Events/FAPAR_CeosWorkshop.php (accessed 1 February 2014).

Chen JM, Liu J, Leblanc SG, Lacaze R, Roujean J-L (2003) Multi-angular optical remote sensing for assessing vegetation structure and carbon absorption. *Remote Sensing of Environment*, **84**, 516–525.

Dai A, Lamb PJ, Trenberth KE, Hulme M, Jones PD, Xie P (2004) The recent Sahel drought is real. *International Journal of Climatology*, **24**, 1323–1331.

Dardel C, Kergoat L, Hiernaux P, Mougin E, Grippa M, Tucker CJ (2014) Re-greening Sahel: 30 years of remote sensing data and field observations (Mali, Niger). *Remote Sensing of Environment*, **140**, 350–364.

Dugas WA, Heuer ML, Mayeux HS (1999) Carbon dioxide fluxes over bermudagrass, native prairie, and sorghum. *Agricultural and Forest Meteorology*, **93**, 121–139.

Eklundh L, Olsson L (2003) Vegetation index trends for the African Sahel 1982–1999. *Geophysical Research Letters*, **30**, 1430.

Eklundh L, Jönsson P, Kuusk A (2007) Investigating modelled and observed Terra/MODIS 500-m reflectance data for viewing and illumination effects. *Advances in Space Research*, **39**, 119–124.

Elberse WT, Breman H (1989) Germination and establishment of Sahelian rangeland species: I. Seed properties. *Oecologia*, **80**, 477–484.

Elberse WT, Breman H (1990) Germination and establishment of Sahelian rangeland species II. Effects of water availability. *Oecologia*, **85**, 32–40.

Falge E, Baldocchi D, Olson R *et al.* (2001) Gap filling strategies for defensible annual sums of net ecosystem exchange. *Agricultural and Forest Meteorology*, **107**, 43–69.

Fensholt R, Sandholt I, Rasmussen MS (2004) Evaluation of MODIS LAI, fAPAR and the relation between fAPAR and NDVI in a semi-arid environment using *in situ* measurements. *Remote Sensing of Environment*, **91**, 490–507.

Fensholt R, Sandholt I, Stisen S (2006) Evaluating MODIS, MERIS, and VEGETATION vegetation indices using *in situ* measurements in a semiarid environment. *IEEE Transactions on Geoscience and Remote Sensing*, **44**, 1774–1786.

Fensholt R, Sandholt I, Proud SR, Stisen S, Rasmussen MO (2010) Assessment of MODIS sun-sensor geometry variations effect on observed NDVI using MSG SEVIRI geostationary data. *International Journal of Remote Sensing*, **31**, 6163–6187.

Fensholt R, Rasmussen K, Kaspersen P, Huber S, Horion S, Swinnen E (2013) Assessing land degradation/recovery in the African Sahel from long-term earth observation based primary productivity and precipitation relationships. *Remote Sensing of Environment*, **5**, 664–686.

Gamon JA, Coburn C, Flanagan LB *et al.* (2010) SpecNet revisited: bridging flux and remote sensing communities. *Canadian Journal of Remote Sensing*, **36**, S376–S390.

Grace J, José JS, Meir P, Miranda HS, Montes RA (2006) Productivity and carbon fluxes of tropical savannas. *Journal of Biogeography*, **33**, 387–400.

Hérault B, Hiernaux P (2004) Soil seed bank and vegetation dynamics in Sahelian fallows; the impact of past cropping and current grazing treatments. *Journal of Tropical Ecology*, **20**, 683–691.

Hiernaux P (1998) Effects of grazing on plant species composition and spatial distribution in rangelands of the Sahel. *Plant Ecology*, **138**, 191–202.

Hiernaux P, Mougin E, Diarra L, Soumaguel N, Lavenu F, Tracol Y, Diawara M (2009) Sahelian rangeland response to changes in rainfall over two decades in the Gourma region, Mali. *Journal of Hydrology*, **375**, 114–127.

Hill MJ, Hanan N (2011) *Ecosystem Function in Savannas: Measurements and Modeling at Landscape to Global Scales*. CRC Press Taylor & Francis, Boca Raton. pp. 559.

Huber S, Tagesson T, Fensholt R (2014) An automated field spectrometer system for studying VIS, NIR and SWIR anisotropy for semi-arid savanna. *Remote Sensing of Environment*, **152**, 547–556.

Hulme M, Doherty R, Ngara T, New M, Lister D (2001) African climate change: 1900–2100. *Climate Research*, **17**, 145–168.

Jones HG, Vaughan RA (2010) *Remote Sensing of Vegetation-Principles, Technigues, and Applications*. Oxford University Press, Oxford. pp. 353.

de Jong R, Schaepman ME, Furrer R, de Bruin S, Verburg PH (2013) Spatial relationship between climatologies and changes in global vegetation activity. *Global Change Biology*, **19**, 1953–1964.

Kim J, Verma SB, Clement RJ (1992) Carbon dioxide budget in temperate grassland ecosystem. *Journal of Geophysical Research*, **97**, 6057–6063.

Kimes DS (1983) Dynamics of directional reflectance factor distributions for vegetation canopies. *Applied Optics*, **22**, 1364–1372.

Kutsch WL, Hanan N, Scholes B, McHugh I, Kubheka W, Eckhardt H, Williams C (2008) Response of carbon fluxes to water relations in a savanna ecosystem in South Africa. *Biogeosciences*, **5**, 1797–1808.

Lambers H, Chapin FS III, Pons T (1998) *Plant Physiological Ecology*. Springer-Verlag, New York, USA. pp. 605.

Lebel T, Cappelaere B, Galle S *et al.* (2009) AMMA-CATCH studies in the Sahelian region of West-Africa: an overview. *Journal of Hydrology*, **375**, 3–13.

Von Maydell HJ (1986) *Trees and Shrubs of the Sahel - Their Characteristics and Uses*. TZ-Verlagsgesellschaft, Rossdorf. pp. 525.

Mbow C, Fensholt R, Rasmussen K, Diop D (2013) Can vegetation productivity be derived from greenness in a semi-arid environment? Evidence from ground-based measurements. *Journal of Arid Environments*, **97**, 56–65.

Merbold L, Ardö J, Arneth A *et al.* (2009) Precipitation as driver of carbon fluxes in 11 African ecosystems. *Biogeosciences*, **6**, 1027–1041.

Moncrieff J, Valentini R, Greco S, Guenther S, Ciccioli P (1997) Trace gas exchange over terrestrial ecosystems: methods and perspectives in micrometeorology. *Journal of Experimental Botany*, **48**, 1133–1142.

Morison JIL, Piedade MTF, Müller E, Long SP, Junk WJ, Jones MB (2000) Very high productivity of the C4 aquatic grass Echinochloa polystachya in the Amazon floodplain confirmed by net ecosystem CO_2 flux measurements. *Oecologia*, **125**, 400–411.

Mougin E, Hiernaux P, Kergoat L *et al.* (2009) The AMMA-CATCH Gourma observatory site in Mali: relating climatic variations to changes in vegetation, surface hydrology, fluxes and natural resources. *Journal of Hydrology*, **375**, 14–33.

Myneni RB, Williams DL (1994) On the relationship between FAPAR and NDVI. *Remote Sensing of Environment*, **49**, 200–211.

Prince SD, Goward SN (1995) Global primary production: a remote sensing approach. *Journal of Biogeography*, **22**, 815–835.

Prince SD, Kerr YH, Goutorbe JP *et al.* (1995) Geographical, biological and remote sensing aspects of the hydrologic atmospheric pilot experiment in the sahel (HAPEX-Sahel). *Remote Sensing of Environment*, **51**, 215–234.

Rasmussen MO, Gottsche FM, Olesen FS, Sandholt I (2011a) Directional effects on land surface temperature estimation from Meteosat second generation for Savanna landscapes. *IEEE Transactions on Geoscience and Remote Sensing*, **49**, 4458–4468.

Rasmussen MO, Göttsche FM, Diop D, Mbow C, Olesen FS, Fensholt R, Sandholt I (2011b) Tree survey and allometric models for tiger bush in northern Senegal and comparison with tree parameters derived from high resolution satellite data. *International Journal of Applied Earth Observation and Geoinformation*, **13**, 517–527.

Roehrig R, Bouniol D, Guichard F, Hourdin F, Redelsperger JL (2013) The present and future of the West African monsoon: a process-oriented assessment of CMIP5 simulations along the AMMA transect. *Journal of Climate*, **26**, 6471–6505.

Samain O, Kergoat L, Hiernaux P, Guichard F, Mougin E, Timouk F, Lavenu F (2008) Analysis of the *in situ* and MODIS albedo variability at multiple time scales in the Sahel. *Journal of Geophysical Research: Atmospheres*, **113 (D14)**, D14119.

Sandmeier S, Muller C, Hosgood B, Andreoli G (1998) Physical mechanisms in hyperspectral BRDF data of grass and watercress. *Remote Sensing of Environment*, **66**, 222–233.

Saunders MJ, Kansiime F, Jones MB (2012) Agricultural encroachment: implications for carbon sequestration in tropical African wetlands. *Global Change Biology*, **18**, 1312–1321.

Sjöström M, Ardö J, Eklundh L *et al.* (2009) Evaluation of satellite based indices for gross primary production estimates in a sparse savanna in the Sudan. *Biogeosciences*, **6**, 129–138.

Stisen S, Sandholt I, Nørgaard A, Fensholt R, Jensen KH (2008) Combining the triangle method with thermal inertia to estimate regional evapotranspiration - Applied to MSG-SEVIRI data in the Senegal River basin. *Remote Sensing of Environment*, **112**, 1242–1255.

Tagesson T, Lindroth A (2007) High soil carbon efflux rates in several ecosystems in southern Sweden. *Boreal Environment Research*, **12**, 65–80.

Tagesson T, Mastepanov M, Tamstorf MP *et al.* (2012) High-resolution satellite data reveal an increase in peak growing season gross primary production in a high-Arctic wet tundra ecosystem 1992–2008. *International Journal of Applied Earth Observation and Geoinformation*, **18**, 407–416.

Tetzlaff G (1983) Albedo of the Sahara. In: *Cologne University Satellite Measurement of Radiation Budget Parameters* (ed. Raschke E), pp. 60–63. Forschungsbericht BMFT, Bonn.

Timouk F, Kergoat L, Mougin E *et al.* (2009) Response of surface energy balance to water regime and vegetation development in a Sahelian landscape. *Journal of Hydrology*, **375**, 12–12.

Trenberth KE, Jones PD, Ambenje P *et al.* (2007) Observations: surface and atmospheric climate change. In: *Climate Change 2007: The Physical Science Basis. Contribution of Working Group I to the Fourth Assessment Report of the Intergovernmental Panel on Climate Change* (ed IPCC), pp. 235–336. Cambridge University Press, Cambridge.

Tucker CJ, Dregne HE, Newcomb WW (1991) Expansion and contraction of the Sahara desert from 1980 to 1990. *Science*, **253**, 299–301.

Veenendaal EM, Kolle O, Lloyd J (2004) Seasonal variation in energy fluxes and carbon dioxide exchange for a broadleaved semi-arid savanna (Mopane woodland) in Southern Africa. *Global Change Biology*, **10**, 318–328.

Verhoef A, Allen SJ, De Bruin HAR, Jacobs CMJ, Heusinkveld BG (1996) Fluxes of carbon dioxide and water vapour from a Sahelian savanna. *Agricultural and Forest Meteorology*, **80**, 231–248.

Supporting Information

Additional Supporting Information may be found in the online version of this article:

Figure S1. Daily values of *in situ* measured normalized difference vegetation index (NDVI) for different viewing angles; (a) NDVI measured at nadir with 60° instantanaeous field of view (IFOV) (black) and hemispherical (gray), (b) NDVI measured at nadir with 60° IFOV (black), measured at 22.5° off-nadir angle toward E with 60° IFOV (blue), measured at 22.5° off-nadir angle toward W with 60° IFOV (red), (c) NDVI measured at nadir with 60° IFOV (black), measured at 45° off-nadir angle toward E with 25° IFOV (blue), measured at 45° off-nadir angle toward W with 25° IFOV (red), and (d) NDVI measured at nadir (black) with 25° IFOV and at 23° off-nadir angle toward NW with 25° IFOV (gray). The NDVI values are the median from between 10:00 and 16:00 hours each day.
Figure S2. Time series 2002 of *in situ* measured effective leaf area index (LAI_e). DOY is day of year.
Figure S3. Time series 2006–2012 of average estimates of (a) aboveground dry biomass (DW), (b) net primary productivity (NPP), and (c) relative water content in the harvested plants (VWC).
Figure S4. Friction velocity (u*) modeled with equation S1 against friction velocity measured by the sonic anemometer.
Figure S5. Density scatter plot for evaluation of gradient estimated sensible heat flux (H) 2010–2012. Half-hourly H measured with the gradient method against half-hourly H measured with the eddy covariance (EC) method. The black line is the one-to-one ratio.
Figure S6. Density scatter plot for evaluation of gradient estimated residuals 2010–2012. Half-hourly residual measured with the gradient method against half-hourly LE measured with the eddy covariance (EC) method. The black line is the one-to-one ratio.
Table S1. Periods during which hydroclimatic variables have been measured 2002–2012 at the Dahra field site. T_{air} and T_{soil} are air and soil temperature, RH is relative humidity, W is wind speed, SWC is soil moisture, and BT is the brightness temperature, G is ground heat flux. Height is measurement height (m) and angle is the sensor view zenith angle (°). Soil moisture was measured in volumetric water content (%). CS215, 107 and A100R are made by Campbell Scientific Inc. (North Logan, USA), ML2X is made by Delta T devices (Cambridge, UK), HFP001 is made by Hukseflux Thermal Sensors B.V. (Delft, Netherlands), ARG1000 is made by Waterra (Burnaby, Canada), the Miniature Infrared (MI) sensors are made by Raytek CO. (Santa Cruz, CA, USA), and the IRTS-P are made by Apogee Electronics (Santa Monica, CA, USA). – means no data.
Table S2. Periods during which reflected and incoming radiation have been measured using different bands and different sensor response configurations 2002–2012. Height is measurement height (m), IFOV is the instantaneous field of view, angle is view angle of the sensor, inc. is incoming, ref. is reflected, trans. is transmitted, NIR is near infrared, PAR is photosynthetically active radiation, irr. is irradiance, Hemi. is hemispherically, Rad. is radiation, Meris is the medium resolution imaging spectroradiometer, MODIS is the moderate resolution imaging spectroradiometer, AVHRR is the advanced very high resolution radiometer, and MSG is the Meteosat Second Generation. SKR1800, SKR1850A, and SKP 215 are made by Skye instruments Ltd. (Llandridod Wells, UK), and SP Lite and NR2Lite is produced by Kipp & Zonen (Delft, The Netherlands).
Table S3. Dominant tree species at Dahra in 2008 and their mean heights and mean diameters at breast height (DBH).
Table S4. Grass and herbaceous species composition at the Dahra field site in 2006, and 2008–2012.
Table S5. Height (m) of the sensors measuring air temperature and wind speed used in the gradient calculations of sensible heat flux. DOY is day of year.